Discover Oncology

Analysis

Identification and Validation of a Novel Lactylation-related Gene Signature to Predict the Prognosis of Endometrial Cancer

Linna Chen[1,2] · Meng Xia[1,2] · Weijia Wen[1,2] · Li Yuan[1,2] · Yan Jia[1,2] · Xueyuan Zhao[1,2] · Haolin Fan[1,2] · Songlin Liu[1,2] · Tianyu Liu[1,2] · Pan Liu[1,2] · Hongye Jiang[1,2] · Wei Wang[1,2] · Yuandong Liao[1,2] · Chunyu Zhang[1,2] · Shuzhong Yao[1,2]

Received: 14 January 2025 / Accepted: 10 May 2025
Published online: 22 May 2025

Abstract

Background Endometrial carcinoma (EC) is a prevalent kind of cancerous tumor with significant morbidity and mortality. Mounting evidence reveals that lactylation modification plays a crucial role in tumorigenesis, but its connection to EC remains poorly understood. This study aimed to identify a lactylation-related gene signature to predict the prognosis of EC.

Methods Differentially expressed lactylation-related genes between EC and normal samples were analyzed using the TCGA database. Univariate and LASSO Cox regression analyses were employed to construct the lactylation-related signature, which was then validated using both the test set and entire set. A nomogram was further developed and evaluated. Additionally, enrichment analysis, immune cell infiltration, tumor mutation burden and drug response were assessed between the two risk groups.

Results Sixteen lactylation-related genes (LRGs) were selected to construct the prognostic signature. Kaplan–Meier survival curves showed that patients in the high-risk group had remarkably worse prognosis. A nomogram based on the signature and other clinical characteristics was constructed and demonstrated strong predictive power. Additionally, biological pathways, immune status, tumor mutation burden and drug response differed between the high- and low-risk groups.

Conclusion In conclusion, our study demonstrated that the LRG signature is a promising biomarker for EC, effectively distinguishing high-risk patients, predicting prognosis, and offering new strategic directions for antitumor immunotherapy.

Keywords Endometrial carcinoma · Lactylation · Gene signature · Prognosis · Immune infiltration · Drug response

Linna Chen, Meng Xia and Weijia Wen contributed equally to the work.

Supplementary Information The online version contains supplementary material available at https://doi.org/10.1007/s12672-025-02663-4.

✉ Yuandong Liao, liaoyd2@mail.sysu.edu.cn; ✉ Chunyu Zhang, zhangchy266@mail.sysu.edu.cn; ✉ Shuzhong Yao, yaoshuzh@mail.sysu.edu.cn | [1]Department of Obstetrics and Gynecology, The First Affiliated Hospital, Sun Yat-Sen University, Guangzhou, Guangdong, People's Republic of China. [2]Guangdong Provincial Clinical Research Center for Obstetrical and Gynecological Diseases, Guangzhou, Guangdong, People's Republic of China.

1 Introduction

Endometrial cancer (EC) is one type of malignant tumor originating from the epithelial cells of the endometrium [1]. It is recognized as the sixth most prevalent cancer among women, whose incidence is estimated to increase to 42.13 per 100,000 people in the US by 2030 [2]. And the morbidity and mortality of EC are increasing worldwide as well [3, 4]. By virtue of the advance in techniques for early diagnosis, patients diagnosed at an early stage account for approximately 75% of EC. Strikingly, the 5-years overall survival rate of patients diagnosed at early stage (stage I) is 74–91% thanks to surgery, while that of advanced-stage (stage III or IV) patients declines to 15–17% owing to a high recurrence rate [3, 5]. In terms of therapeutic approaches for endometrial cancer, adjuvant therapies, including chemotherapy and radiotherapy, might benefit patients as well as surgery. But therapeutic options beyond first-line chemotherapy remain limited [6, 7]. Hence, exploration and identification of novel biomarkers is crucial to help screen out patients with poor prognosis and tailor their treatment strategies accordingly, ultimately improving clinical outcomes and survival rates.

Protein lactylation has emerged as a novel lactate-mediated post-translational modification of both histone and non-histone proteins, first reported in 2019 [8]. Similar to methylation, lactylation involves the addition or removal of lactic acid groups to lysine residues, a process mediated by lactyltransferases and delactylases [9–12]. Furthermore, histone lactylation participates in numerous biological and pathological processes. Mounting studies have illustrated that histone lactylation plays a crucial part in neurodevelopment [13], inflammation, macrophage polarization, regulation of tumor proliferation [14] and other glycolysis-related cellular functions [8]. Since aerobic glycolysis is an important source of lactic acid for lactylation in cancers and is closely linked to the onset and progression of tumors, an increasing number of relevant researches have proliferated to explore the role of lactylation and its clinical value in several kinds of cancers [15]. Numerous studies have shown that patients with higher levels of lactylation suffer from worse prognosis in different cancers. Mechanistically, the tumor metabolite lactate in the tumor microenvironment (TME) could regulate protein lactylation, subsequently regulating gene expression, metabolic reprogramming, and immune response, which is of great value in tumorigenesis, as it influences key processes such as cell proliferation, survival, and immune evasion, contributing to the progression and malignancy of tumors [8, 16–18]. Even though lactylation has attracted broad attention, relevant research on its role in endometrial cancer is still limited, especially regarding the signatures that can be used to assess the prognostic significance of lactylation-related genes (LRGs) in EC. This gap highlights the need for further investigation into how lactylation and LRGs contribute to the progression of EC and how these molecular markers can be used to predict patient outcomes and guide treatment strategies.

In our study, we collected the lactylation-related data published thus far and conducted an analysis of these genes in EC patients, utilizing data obtained from The Cancer Genome Atlas (TCGA) database, a comprehensive resource that profiles the molecular characteristics of various types of cancer. Then, we constructed a 16-gene lactylation-related signature using LASSO analysis. We further explored the effects of this signature on prognosis, biological functions, immune cell infiltration and drug sensitivity. Notably, our findings demonstrated that the lactylation-related signature held promise as a predictive factor for the prognosis of EC patients and their response to treatment, which opens avenues for future research and clinical applications.

2 Materials and methods

2.1 Acquisition of expression profiles and clinical data of EC patients

The expression and clinical data of EC patients were downloaded from the TCGA database (https://portal.gdc.cancer.gov/). 537 cancer cases and 35 normal samples were initially selected to identify the differentially expressed genes (DEGs). We excluded patients who had incomplete clinical and follow-up information to ensure the reliability and completeness of our analysis. Finally, 525 cancer samples and 35 normal samples were eventually included in the subsequent studies. The clinical features are detailed in Table 1. All transcriptomic data were standardized and normalized, and DEGs were analyzed using "DESeq2" package. The DEGs threshold was set as follows: adjusted P value < 0.05. A volcano Plot was generated using the "ggplot2" package to visually represent the differentially expressed genes.

Table 1 Clinical features of 560 samples

Covariates	Type	Entire set N (percentage)	Train set N (percentage)	Test set N (percentage)
Survival status	Alive	445 (84.76%)	225 (85.55%)	220 (83.97%)
	Dead	80 (15.24%)	38 (14.45%)	42 (16.03%)
Age	< 65	283 (53.90%)	146 (55.51%)	137 (52.29%)
	>= 65	242 (46.10%)	117 (44.49%)	125 (47.71%)
Stage	Stage I and Stage II	375 (71.43%)	182 (69.20%)	193 (73.66%)
	Stage III and Stage IV	150 (28.57%)	81 (30.80%)	69 (26.34%)
Grade	G1 and G2	214 (40.76%)	110 (41.83%)	104 (39.69%)
	G3 and high grade	311 (59.24%)	153 (58.17%)	158 (60.31%)

2.2 Assertion of lactylation-related genes in EC

The lactylation-related genes were gathered from previously published studies [8, 9, 19]. After deleting duplicated genes, we identified a total gene set of 332 genes, which were presented in Additional file 2: Table S1. A heatmap was generated with the "pheatmap" package to visualize the lactylation-related DEGs.

2.3 Functional enrichment analysis

To explore the potential biological functions of the lactylation-related differentially expressed genes (LRDEGs), we implemented the "ClusterProfiler" package in R software for Gene Ontology (GO) term enrichment analysis, which included three categories: biological process (BP), molecular function (MF), cellular component (CC) as well as the Kyoto Encyclopedia of Genes and Genomes (KEGG) pathway enrichment analysis.

2.4 Construction and validation of a lactylation-related prognosis signature

525 cancer samples (entire set) were randomly allocated to the train set (n = 263) and test set (n = 262) in a one-to-one ratio. The test set and the entire set were used for validation. First, we utilized the univariate Cox regression in the train set to identify candidate survival-related LRDEGs with significance level of $p < 0.05$. Next, LASSO regression analysis was used to screen out genes involved in the prediction signature in train set; P value < 0.05 was considered statistically significant. The least absolute shrinkage and selection operator (LASSO) was used to construct the lactylation-related prognosis signature, with the risk score signature developed from the training set data as follows: $\text{Riskscore} = \Sigma_{i=1}^{N}(\exp \times \text{coefficient})$ where N is the number of signature genes, exp represents the gene expression value of each gene and coefficient refers to the coefficient index. We treated the median risk score in the train set as the cutoff value and patients from the train set were divided into two groups. Kaplan–Meier analysis was conducted to evaluate overall survival (OS) differences between the two groups. The receiver operating characteristic (ROC) curve was generated using the R package "timeROC" to evaluate the sensitivity and specificity of the risk signature. Principal component analysis (PCA) and t-distributed stochastic neighbor embedding analysis (t-SNE) were performed using the R packages "stats" and "Rtsne" to examine the distribution and outcome of high-risk and low-risk group patients. The test set and the entire set were used to validate the signature.

2.5 Independent prognostic analysis and construction of a nomogram

Univariate and multivariate Cox regression analyses were performed using the "survival" package in R to examine the relationship between prognosis, risk score, age, grade and stage. Then, we developed a nomogram using the "survival" and "rms" R packages to predict 1-, 3-, and 5-year survival rates for EC patients. ROC curves, decision curve analysis (DCA), and calibration curves were employed to evaluate the signature's performance.

2.6 Gene set enrichment analysis

Gene set enrichment analysis (GSEA) [20] was utilized using the "clusterProfiler" package to explore the molecular mechanisms underlying the risk signature. The annotated gene sets for GSEA were obtained from Hs.entrez.v7.0 of the Molecular Signature Database (MsigDB) (https://www.gsea-msigdb.org/gsea/msigdb/). We separated the samples in the entire set into the high- and low-risk groups based on scores calculated by the signature, and then compared the enriched pathways between the two groups.

2.7 Analysis of the tumor immune microenvironment (TIME), tumor-infiltrating immune cells (TIICs), immune checkpoint and immunophenotype score (IPS)

ESTIMATE was used to assess the relationship between the risk signature and the tumor microenvironment (TME), including the stromal score, immune score, tumor purity, and ESTIMATE score [21, 22]. To seek the relationships between the risk signature and immune status, differences in immune infiltrating cells between the two risk groups were analyzed and compared using CIBERSORT and single-sample Gene Set Enrichment Analysis (ssGSEA) [23]. Next, we compared the expression levels of 33 immune checkpoint genes in the two risk groups. Using the "survival" and "survminer" packages, we conducted joint survival analysis of the expression of PD-1, CTLA-4 and risk score, respectively. The immunophenotype scores (IPS) were used as a predictive measure to estimate a patient's response to immune checkpoint inhibitor-based immunotherapy. IPS values for EC patients were obtained from The Cancer Immunome Atlas (TCIA) database (https://tcia.at/home), and we compared the IPS values between the two risk groups.

2.8 Analysis of tumor mutation burden (TMB), Microsatellite instability (MSI) and drug inference

The mutation data collected from TCGA were analyzed using the R package "maftools", which facilitated the visualization and interpretation of somatic mutations in the context of the risk signature and their association with the clinical features of the samples. And we calculated TMB by the formula: TMB = (total mutation/total covered bases) * 10^6. Microsatellite instability (MSI) status for each sample was also collected from TCGA. We then conducted joint survival analysis of the TMB, MSI and risk score respectively, using the "survival" package and the "survminer" package. In the pursuit of identifying potentially effective therapeutic agents between risk groups, the predictive capabilities provided by the "oncoPredict" R package were extensively utilized, which allowed for the prediction of drug responses based on gene expression profiles, helping to identify potential therapeutic agents that could be effective for patients in each risk group [20].

2.9 Data analysis

All statistical analyses were performed using the R (version 4.3.3) software. P values < 0.05 were considered significant, with the following significance levels: *P < 0.05, **P < 0.01, and ***P < 0.001.

3 Results

3.1 Identification of LRGs in EC

The flow chart of the study is shown in Fig. 1. First, we used the DESeq2 algorithm to identify the DEGs in EC. By comparing tumor tissues with normal tissues, 12,001 DEGs were identified, including 6919 upregulated and 5082 downregulated genes. The results were visualized in a volcano plot, highlighting the distribution of these genes based on their statistical significance and fold change (Fig. 2A). The intersection genes between DEGs and the lactylation-related genes were identified using a Venn diagram (Fig. 2B). These genes were then further analyzed, and their expression profiles were visualized using a heatmap (Fig. 2C), which provided a clear representation of the expression patterns across different samples and groups. In exploring the functions of the 212 lactylation-related DEGs through GO enrichment analysis, we first identified that these genes were involved in some pathways such as RNA splicing (Fig. 2D). This finding suggests that lactylation may play a role in regulating RNA processing and splicing mechanisms, which could contribute to the

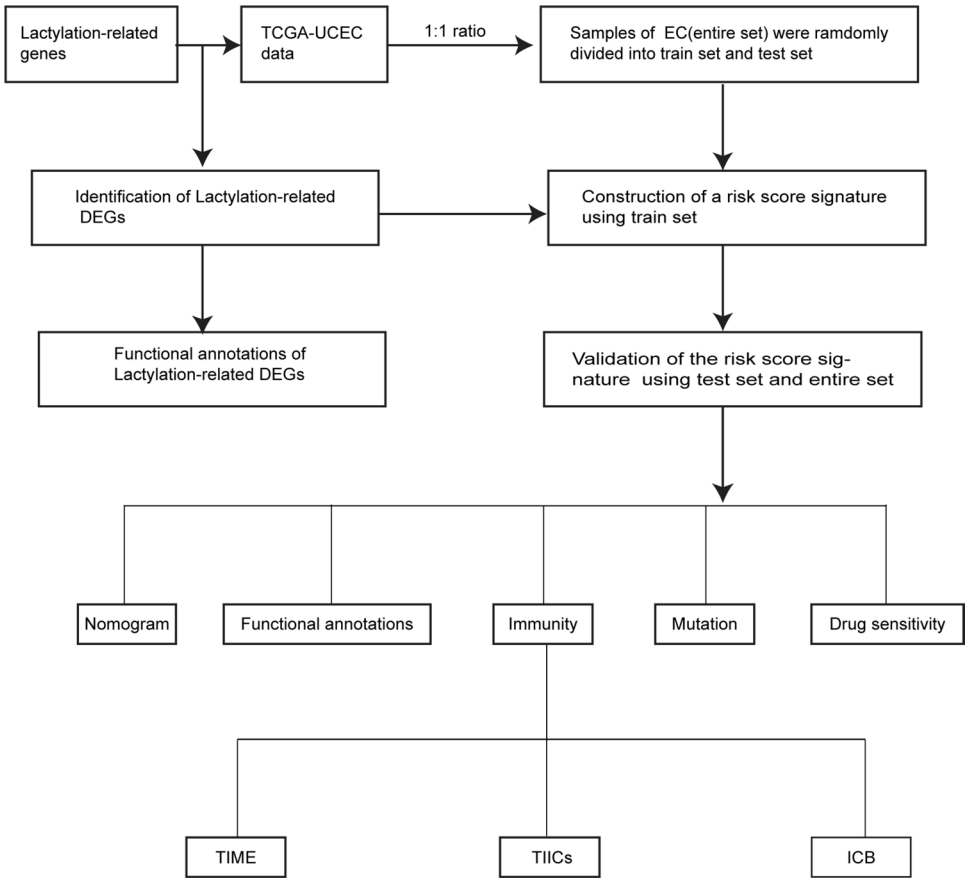

Fig. 1 Flow chart of this study. TCGA, The Cancer Genome Atlas; UCEC, uterine corpus endometrial carcinoma; DEGs, differentially expressed genes; EC, endometrial carcinoma; TIME, tumor immune microenvironment; TIICs, tumor immune infiltrating cells; ICB, immune checkpoint blockade

pathogenesis of endometrial cancer. In KEGG enrichment analysis, we found that these lactylation-related differentially expressed genes were substantially associated with glycolysis (Fig. 2E). This hints that lactylation may play a crucial part in the regulation of metabolic pathways, particularly glycolysis, in endometrial cancer. This association with glycolysis highlights the potential metabolic reprogramming in cancer cells, where lactylation could influence energy production and tumor progression.

3.2 Establishment of a lactylation-associated gene prognostic signature in EC

The entire set was randomly divided into a train set and a test set in a 1:1 ratio. First, in the train set, univariate Cox regression was conducted to screen out prognostic-related genes from above the previously identified lactylation-related differentially expressed genes (Additional file 1: Fig. S1). Following this, these genes were subjected to LASSO Cox regression analysis (Fig. 3A, B), which further refined the selection of genes based on their predictive value. Ultimately, 16 genes were selected and formed the foundation of a risk signature. This risk signature was established using the following formula: riskscore = NOP2 × 0.252 + HSPE1 × 0.020 + HIST1H1C × 0.028 + BZW2 × 0.413—HIST1H3A × 0.479—PFN1 × 0.139 + ACAT2 × 0.046 -TP53 × 0.024 + EMG1 × 0.550 + GFAP × 0.514 + SIRT2 × 0.371 + PRKDC × 0.181—LGALS1 × 0.078 + RIMS1 × 3.877—SIRT3 × 0.878- VIM × 0.167. After calculating the risk scores for each sample in the train set, the samples were divided into two groups: a high-risk group and a low-risk group. This division was based on the median risk score (Fig. 3C). The Kaplan–Meier survival analysis illustrated high-risk patients suffered from worse survival outcomes while low-risk patients showed notably higher OS (Fig. 3E). Moreover, t-distributed stochastic neighbor embedding (t-SNE), principal component analysis (PCA), and Receiver Operating Characteristic curve (ROC) were conducted to evaluate the robustness and predictive power of the risk signature from various perspectives. As shown in Fig. 3F, G, the t-SNE and PCA analyses effectively distinguished patients into two distinct risk groups, confirming the ability of this 16-gene risk signature to stratify patients based on their prognosis. Strikingly, the ROC curve analysis demonstrated the excellent predictive efficiency of the signature. The area under the curve (AUC) for predicting 1-year, 3-year, and 5-year overall survival (OS) reached 0.829, 0.912, and 0.878 respectively, indicating the strong ability of the risk signature to

Fig. 2 Screening and functional analysis of lactylation-related genes in EC. **A** Volcano plots of the differentially expressed genes (DEGs) in ▶ TCGA-UCEC. **B** Venn diagram showing 212 lactylation-related differentially expressed genes (LRDEGs). **C** Heatmap presenting the expression level of 212 lactylation-related differentially expressed genes (LRDEGs). **D** GO functional enrichment of 212 lactylation-related differentially expressed genes (LRDEGs). **E** KEGG pathways enrichment of 212 lactylation-related differentially expressed genes (LRDEGs)

predict patient survival over different time intervals. These results highlight the potential of this signature as a powerful tool for prognostic prediction in endometrial cancer.

3.3 Validation of the lactylation-associated genes prognostic signature in EC

As described above, the test set and the entire set were applied to further verify the accuracy and confidence of this signature. In accordance with the preceding formula, patients in the test set were assigned their corresponding risk scores and the median was used to distinguish the high- and low- risk groups. The same process was performed on the entire set. Figure 4A, B exhibited the distribution of risk scores and survival status of patients across different groups. PCA and t-SNE results confirmed the signature's ability to differentiate between the two risk groups (Fig. 4C–F). And the overall survival of high-risk patients notably declined compared to low-risk patients in both validation sets which is consistent with the training set (Fig. 4G, H). Additionally, ROC curve analysis was applied to assess the accuracy of this signature in both sets (Fig. 4I, J). All above results strongly confirmed that this lactylation-related gene signature is reliable in predicting prognosis of endometrial patients.

3.4 Validation of the signature as an independent prognostic factor

The results of univariate and multivariate analyses demonstrated that the signature could serve as an independent prognostic factor for EC patients. The hazard ratio (HR) for this signature was 1.888 (95% confidence interval (CI), 1.604–2.223) in univariate regression analysis and reached 1.580 (95% CI, 1.287–1.939) in multivariate regression analysis. Both were statistically significant (Fig. 5A, B). For clinical application, we constructed a nomogram incorporating risk score, patient age, tumor grade, and tumor stage (Fig. 5C). A calibration curve was used to assess the predictive accuracy of the nomogram and showed a close match between the predicted and observed outcomes (Fig. 5D). Decision curve analysis demonstrated that the nomogram provided greater clinical benefits compared to prognostic estimates based solely on clinical characteristics (Fig. 5E). Moreover, the ROC curve revealed that our nomogram performed well in differentiating the outcomes, with AUC values for the 1-, 3-, and 5-year predictions of 0.850, 0.929, and 0.894, respectively (Fig. 5F). These results demonstrated the robustness of the nomogram in predicting overall survival. Consequently, we conclude that the lactylation score may serve as a reliable independent prognostic indicator for EC.

3.5 Functional enrichment analysis based on the risk signature

To examine potential differences in the functional characteristics of the signature, functional enrichment analysis was conducted on the groups categorized by risk. The GO enrichment analysis revealed a notable increase in small GTPase-mediated signal transduction, positive regulation of protein localization, mitotic cell cycle phase transition and other related processes (Fig. 6A). Furthermore, the KEGG pathway analysis revealed significant enrichment in the cell cycle, DNA replication, and focal adhesion (Fig. 6B). Additionally, we also employed GSEA to analyze the transcript profiles of patients in different risk groups. The high-risk group was demonstrated to be strongly linked with E2F targets, G2M checkpoint and MYC targets according to GSEA analysis (Fig. 6C).

3.6 Investigation of immune factors and immunotherapeutic response in risk groups

We subsequently explored the correlation between lactylation-related risk score (LRRS) and immune features. The association between LRRS and the TIME was assessed using the stromal score, immune score, ESTIMATE score and tumor purity. Figure 7A revealed LRRS is negatively correlated with immune status and positively correlated with tumor purity. CIBERSORT and ssGSEA were then applied to further explore immunity levels in different risk groups. The heatmap illustrated the immune infiltration landscape distinguishing the two subgroups (Fig. 7B). Moreover, the distribution of immune infiltrating cells was markedly different in two groups (Fig. 7C). More specifically, the abundance of B cells, CD8 + T cells, DCs, Macrophages, Mast cells, NK cells, Th1 cells and Th17 cells was higher in the low-risk group while CD4 + T cells were

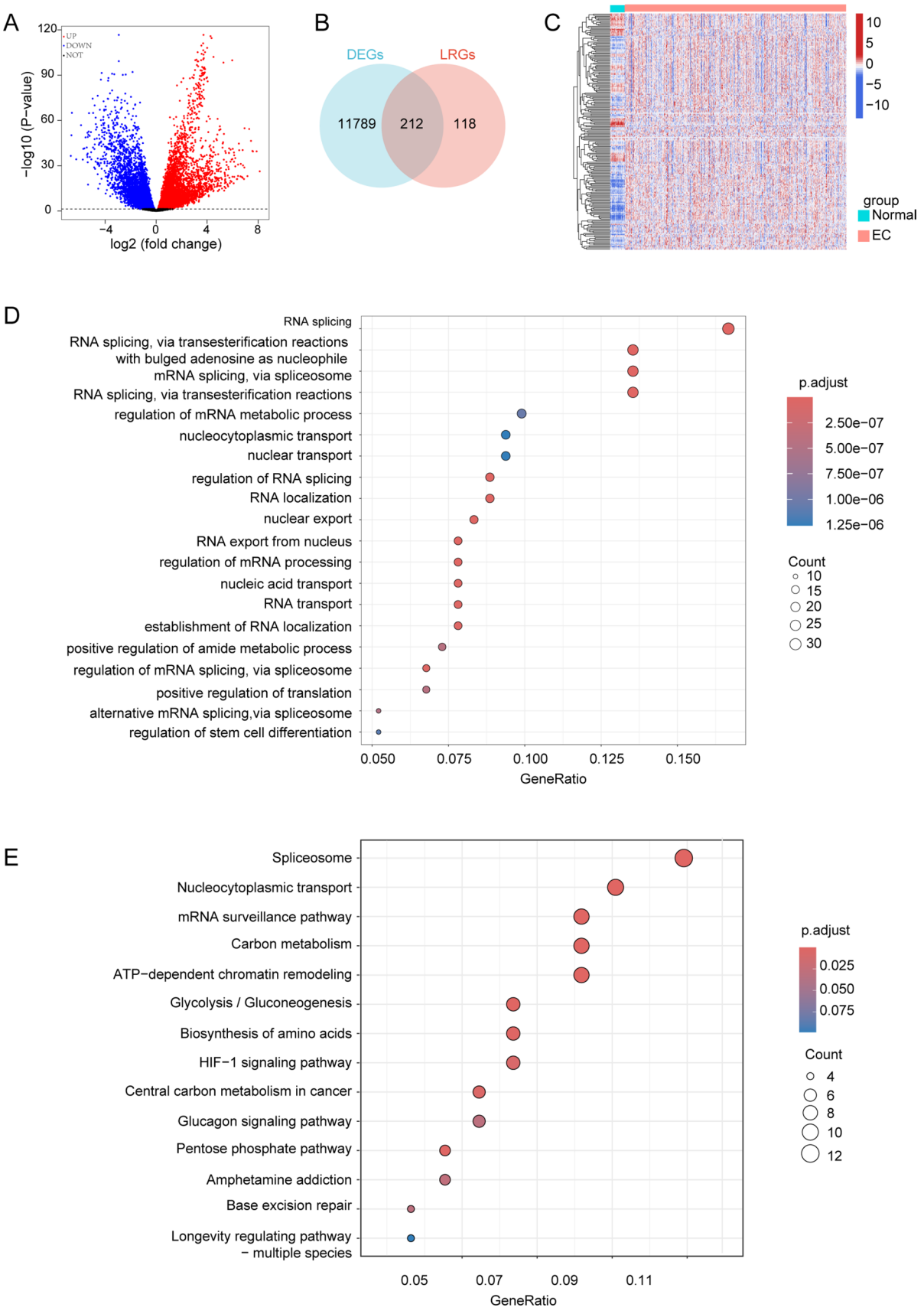
A
UP
DOWN
NOT
−log10 (P−value)
log2 (fold change)
B
DEGs
LRGs
11789
212
118
C
10
5
0
−5
−10
group
Normal
EC
D
RNA splicing
RNA splicing, via transesterification reactions with bulged adenosine as nucleophile
mRNA splicing, via spliceosome
RNA splicing, via transesterification reactions
regulation of mRNA metabolic process
nucleocytoplasmic transport
nuclear transport
regulation of RNA splicing
RNA localization
nuclear export
RNA export from nucleus
regulation of mRNA processing
nucleic acid transport
RNA transport
establishment of RNA localization
positive regulation of amide metabolic process
regulation of mRNA splicing, via spliceosome
positive regulation of translation
alternative mRNA splicing,via spliceosome
regulation of stem cell differentiation
GeneRatio
p.adjust
2.50e−07
5.00e−07
7.50e−07
1.00e−06
1.25e−06
Count
10
15
20
25
30
E
Spliceosome
Nucleocytoplasmic transport
mRNA surveillance pathway
Carbon metabolism
ATP−dependent chromatin remodeling
Glycolysis / Gluconeogenesis
Biosynthesis of amino acids
HIF−1 signaling pathway
Central carbon metabolism in cancer
Glucagon signaling pathway
Pentose phosphate pathway
Amphetamine addiction
Base excision repair
Longevity regulating pathway − multiple species
GeneRatio
p.adjust
0.025
0.050
0.075
Count
4
6
8
10
12

Fig. 3 Establishment of lactylation-related gene prognostic signature. **A**, **B** LASSO coefficient profiles and cross-validation via minimum criteria generating 16 significant prognostic LRGs. **C** Distribution of risk scores in the train set. **D** Kaplan–Meier survival curves showing the significant differentiation in overall survival of patients between two risk subgroups in the train set. **E** Distribution of survival status with an increasing risk score in the train set. **F**, **G** Principal component analysis and t-Distributed stochastic neighbor embedding analysis between two risk subgroups in the train set. **H** ROC curves evaluating the predictive accuracy of the signature in predicting 1-, 3-, and 5-year OS in the train set

more abundant in the high-risk group. To evaluate the potential treatment effect of immune checkpoint inhibitors (ICIs), we probed into the relationship between 33 ICIs and the signature (Fig. 7D). The result showed that the expression of immunotherapy markers, such as PD-1 and CTLA-4, were higher in low-risk patients. Figure 7E further confirmed that low-risk patients had a higher response rate to ICIs. Additionally, we conducted conjoint survival analysis between lactylation score groups and PD-1 as well as CTLA4, which revealed statistical differences (Fig. 7F, G). Above findings implied that the signature could assist in screening patients who might benefit from immune checkpoint blockade therapy.

3.7 Relationship between tumor mutation burden, microsatellite instability and risk score

Proto-oncogene mutation is well-established as an important cause of tumorigenesis. We thus analyzed the mutation profiles of two risk groups in order to dig out the relevance between lactylation and tumor mutation. We found that a higher percentage of patients in the low-risk group (97.64%) had gene mutations compared to the high-risk group (97.46%). In terms of specific mutations, the gene with the highest mutation frequency in the high-risk group was TP53, while PTEN had the highest mutation frequency in the low-risk group. Interestingly, the dominant mutation type in both groups was missense mutations (Fig. 8A, B). These findings suggest a potential relationship between lactylation and specific proto-oncogene mutations, which could provide further insights into the molecular mechanisms driving tumorigenesis in different risk groups. The observation that different genes, such as TP53 and PTEN, dominate in each risk group might also reflect distinct pathways or mechanisms associated with tumor development in these populations. The analysis of tumor mutation burden (TMB) values in patients revealed an important finding: patients with low TMB values had a less favorable prognosis, as shown in Fig. 8C. This suggests that a lower TMB may be linked to more aggressive tumor behavior or resistance to certain treatments, highlighting the potential importance of TMB in predicting patient outcomes. Furthermore, the conjoint survival analysis using both TMB values and lactylation risk scores (Fig. 8D) provided deeper insight into their combined impact on the prognosis of endometrial cancer. The results indicated that both TMB and risk scores are significant factors that can influence the prognosis of EC patients, reinforcing the idea that molecular markers like TMB and lactylation could play a crucial role in predicting the clinical outcomes and guiding treatment strategies. Moreover, the combination of TMB and lactylation risk scores might provide a more comprehensive understanding of the tumor microenvironment and its response to therapies, especially immune checkpoint inhibitors (ICIs). This could ultimately lead to better patient stratification and more tailored therapeutic approaches. Following the investigation into TMB, we also examined microsatellite instability (MSI) scores in different risk groups. Figure 8E, F clearly showed that low-risk patients exhibited higher MSI (microsatellite instability) scores compared to high-risk patients. This suggests that MSI could be a relevant factor in differentiating between these two risk groups, potentially influencing the molecular characteristics and behavior of the tumors in each group. Besides, Fig. 8G showed that patients in the MSI group had better survival rates compared to those in the microsatellite stable (MSS) group. This aligns with the growing body of evidence suggesting that MSI-H tumors are often more responsive to immune checkpoint inhibitors and may have better prognoses due to their heightened immune response. In Fig. 8H, a conjoint analysis was performed using both MSI status and lactylation risk scores. The results indicated that both MSI and lactylation significantly impact the prognosis of endometrial cancer. This emphasizes that lactylation, in combination with MSI, could provide valuable insights for predicting the clinical outcomes of EC patients, potentially influencing treatment decisions, particularly for therapies that target the immune system. All these findings suggest that integrating MSI and lactylation risk scores could enhance prognostic accuracy, guiding treatment strategies more effectively, especially in the context of immunotherapies.

3.8 Drug sensitivity

EC patients could benefit from the selection of appropriate drugs for comprehensive treatment. To enhance the precision of treatment strategies for endometrial cancer patients, we focused on evaluating the patients' responses to various oncology drugs based on their risk group classification. The "oncoPredict" package was utilized to predict the half-maximal inhibitory concentration (IC50) values of different anticancer drugs for each patient, which helps assess

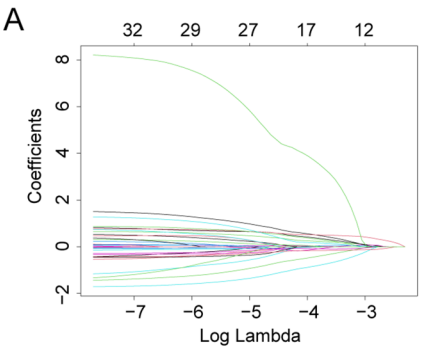
A
32 29 27 17 12
Coefficients
Log Lambda

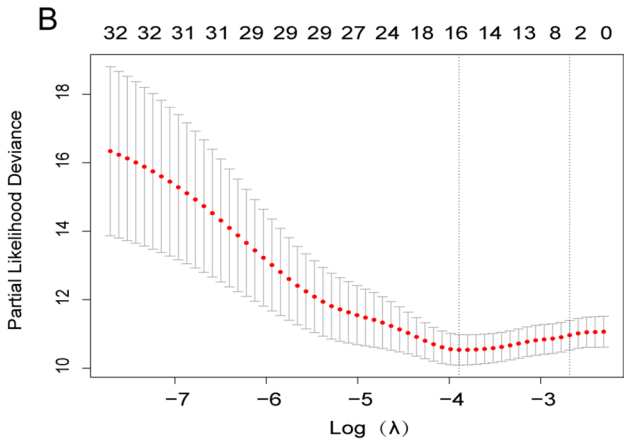
B
32 32 31 31 29 29 29 27 24 18 16 14 13 8 2 0
Partial Likelihood Deviance
Log (λ)

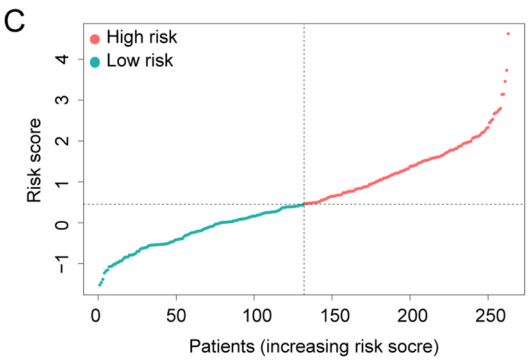
C
High risk
Low risk
Risk score
Patients (increasing risk socre)

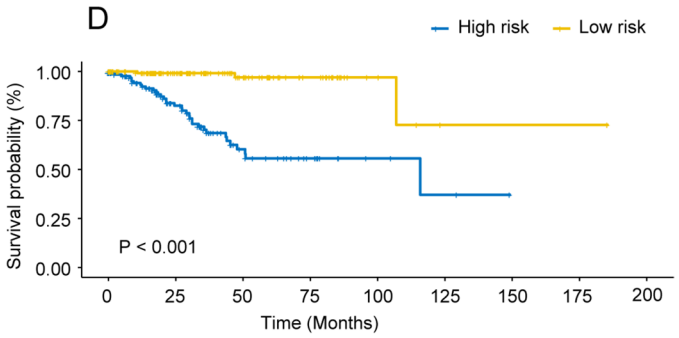
D
High risk
Low risk
Survival probability (%)
P < 0.001
Time (Months)

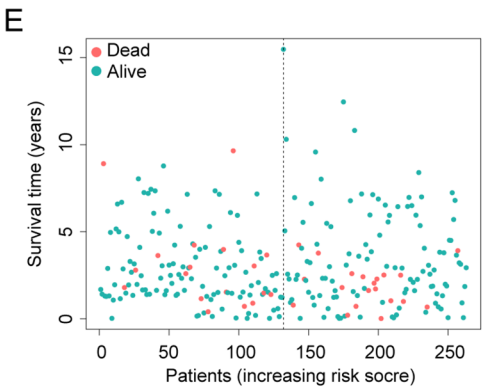
E
Dead
Alive
Survival time (years)
Patients (increasing risk socre)

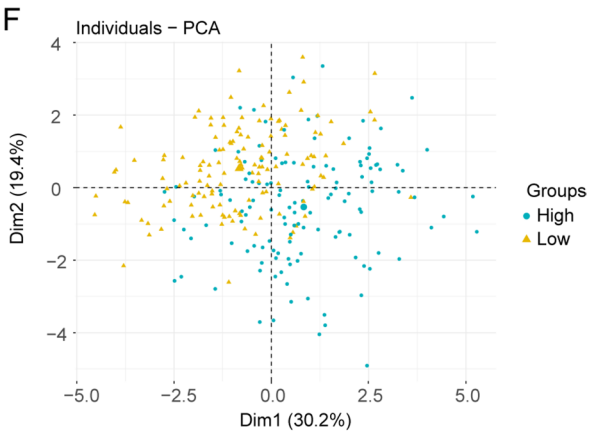
F
Individuals – PCA
Dim2 (19.4%)
Dim1 (30.2%)
Groups
High
Low

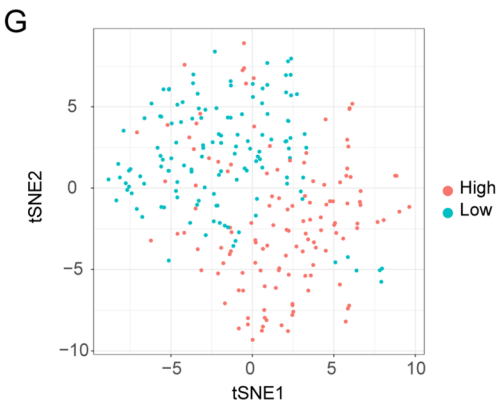
G
tSNE2
tSNE1
High
Low

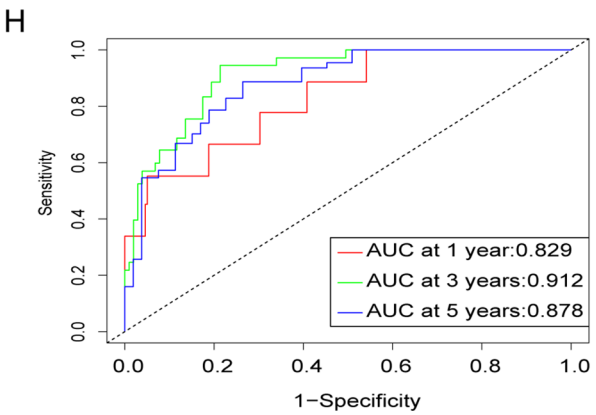
H
Sensitivity
1−Specificity
AUC at 1 year:0.829
AUC at 3 years:0.912
AUC at 5 years:0.878

Fig. 4 Validation of lactylation-related gene prognostic signature. **A**, **B** The distribution of risk scores and survival status of patients between two risk subgroups in the test set (**A**) and entire set (**B**). **C**, **D** Principal component analysis between two risk subgroups in the test set (**C**) and entire set (**D**). **E**, **F** T-Distributed stochastic neighbor embedding analysis between two risk subgroups in the test set (**E**) and entire set (**F**). **G**, **H** Kaplan–Meier survival curves verifying the significant differentiation in OS of patients between two risk subgroups in the test set (**G**) and entire set (**H**). **I**, **J** ROC curve of 1, 3, 5-years survival prediction in the test set (**I**) and entire set (**J**)

the sensitivity of tumors to specific treatments. The results, shown in Fig. 9, revealed significant differences in the IC50 values between the two risk groups, indicating that the risk profiles influence drug sensitivity. In particular, high-risk patients were more sensitive to paclitaxel, olaparib, and MK.1775. This suggests that these patients may benefit more from therapies involving these drugs, which could be particularly useful in targeting tumors with specific molecular characteristics. Low-risk patients, on the other hand, responded better to platin, tamoxifen, bleomycin, cyclophosphamide, sunitinib, and oxaliplatin. This highlights the potential efficacy of these drugs in patients with lower-risk profiles, suggesting that tailored therapies could optimize treatment outcomes. All of these findings underscore the importance of personalized medicine, where the risk profile of a patient guides the selection of the most effective chemotherapy or targeted therapy. Moreover, understanding how different risk groups respond to specific oncology drugs can significantly improve treatment strategies and outcomes for EC patients.

4 Discussion

In the past decades, the morbidity of EC has been rapidly increasing year by year owing to the following factors: an ageing population, the growing prevalence of obesity and some reproductive risk factors that increase lifetime exposure to unopposed oestrogen resulting from early menarche, late menopause, PCOS, and nulliparity [24]. The increasing in the mortality rate remained sharper than that of morbidity. And the increased rate of advanced-stage and high-risk histology cancers as well as rising age at diagnosis might explain this trend to some extent [5, 25]. Due to the development of early diagnostic techniques, the overall survival rate of endometrial cancer has improved dramatically recently [26]. However, the remaining 15% of patients diagnosed at an advanced stage showed a poor prognosis [27]. And more effort is still needed to deal with the recurrence and metastasis of these patients [28]. Radical hysterectomy is considered the standard treatment for patients diagnosed at an early stage, and adjuvant treatments including chemotherapy, radiotherapy and immunotherapy are required for high-risk patients [29, 30]. The 5-year survival rate of patients diagnosed early is favorable if they undergo surgical intervention and receive adjuvant radiation and chemotherapy. However, there are limited therapeutic options for patients diagnosed as high-risk especially those with recurrent or metastatic disease which might lead to the unsatisfactory prognosis [31]. Therefore, it is of great value to explore in depth the prognostic biomarkers and therapeutic targets for endometrial cancer patients.

Lactate, once considered a metabolic waste product, has been verified to play an essential role in providing nutrients for tumor cells and promoting the growth, proliferation, metastasis of tumor cells. Mechanistically, lactate could promote tumor metabolic reprogramming, reconfigure tumor microenvironment and directly influence a wide variety of kinds of immune cells which contributes to the immunosuppression and drug resistance of cancer. For instance, lactate could create an acidic tumor microenvironment whose pH ranges from 6.0 to 6.5, consequently promoting processes like metastasis, angiogenesis and immunosuppression and tumor resistance [32, 33]. More importantly, in 2019 researchers from the University of Chicago discovered for the first time the role of lactate played in epigenetic modification, which referred to as protein lactylation [7]. Soon the role of lactylation in the occurrence and progression of tumors has attracted a great deal of attention. And numerous studies have clarified the oncogenic effect of this novel posttranslational modification. As to the field of bioinformatics, there have been several lactylation-related signatures to predict the prognosis of cancer patients including hepatocellular carcinoma, pancreatic adenocarcinoma, and colorectal cancer [34–37]. Nonetheless, research to elucidate the role of lactylation in endometrial cancer remains quite limited. The relationship between lactylation-related genes and endometrial cancer prognosis is still in a blurred situation.

To investigate the function of EC lactylation modification, we explored LRGs and their potential biological functions, then constructed a lactylation-related signature that can predict prognosis and therapy response for endometrial cancer patients. In particular, the expression level of lactylation-related genes obtained from previously published studies was first analyzed using TCGA-UCEC cohort. Then 212 lactylation-related DEGs were screened which were inextricably linked to important pathways in cancers such as pentose phosphate pathway [38] and HIFs and NRF2 signaling [39]. Afterwards we split the entire cohort in half randomly. 35 DEGs were identified to be associated with

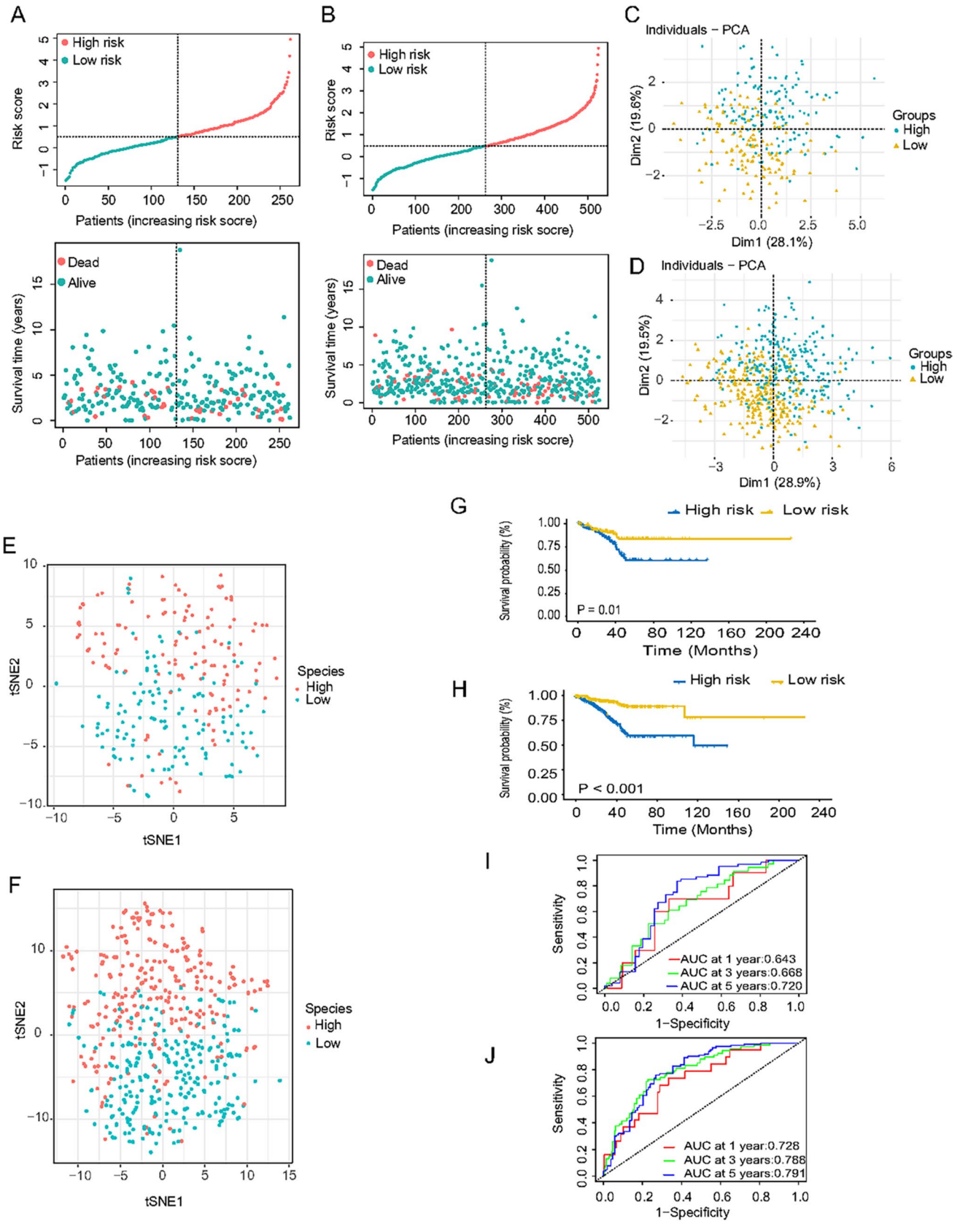
A
High risk
Low risk
Risk score
Patients (increasing risk socre)
Dead
Alive
Survival time (years)
Patients (increasing risk socre)
B
High risk
Low risk
Risk score
Patients (increasing risk socre)
Dead
Alive
Survival time (years)
Patients (increasing risk socre)
C
Individuals – PCA
Dim2 (19.6%)
Dim1 (28.1%)
Groups
High
Low
D
Individuals – PCA
Dim2 (19.5%)
Dim1 (28.9%)
Groups
High
Low
E
tSNE2
tSNE1
Species
High
Low
F
tSNE2
tSNE1
Species
High
Low
G
High risk
Low risk
Survival probability (%)
P = 0.01
Time (Months)
H
High risk
Low risk
Survival probability (%)
P < 0.001
Time (Months)
I
Sensitivity
1−Specificity
AUC at 1 year:0.643
AUC at 3 years:0.668
AUC at 5 years:0.720
J
Sensitivity
1−Specificity
AUC at 1 year:0.728
AUC at 3 years:0.788
AUC at 5 years:0.791

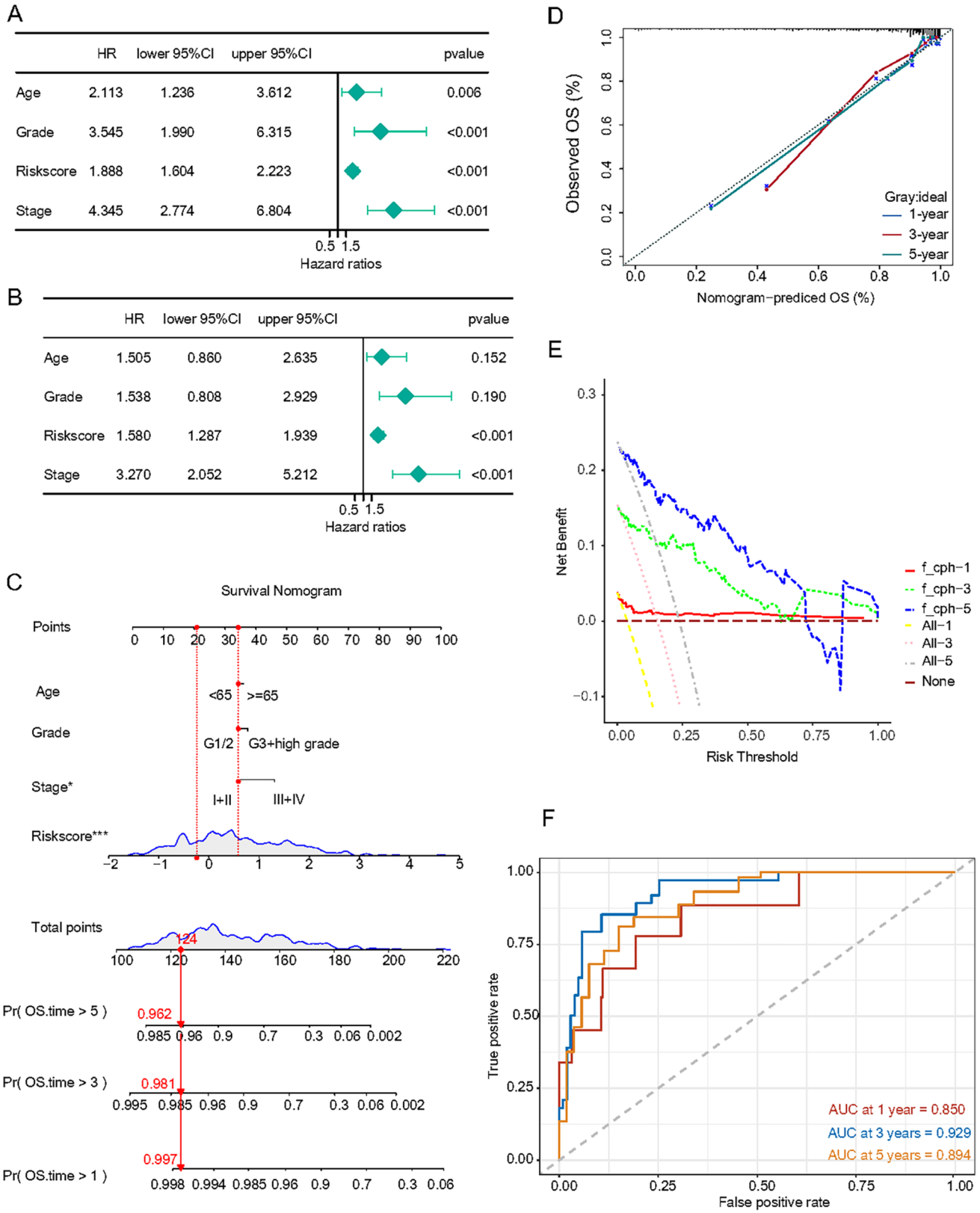

Fig. 5 Assessment of the LRGs prognostic signature in EC. **A**, **B** Univariate (**A**) and multivariate (**B**) Cox analyses of risk score and clinicopathologic factors in the entire set. **C** Clinical prognostic nomogram considering the risk score, age, grade and stage to predict 1-, 3-, and 5-year OS in the entire set. **D** Calibration curves showing the observed and actual 1-, 3-, and 5-year OS. **E** DCA showing the clinical benefits of the nomogram. **F** ROC curves showing the prognostic accuracy of nomogram

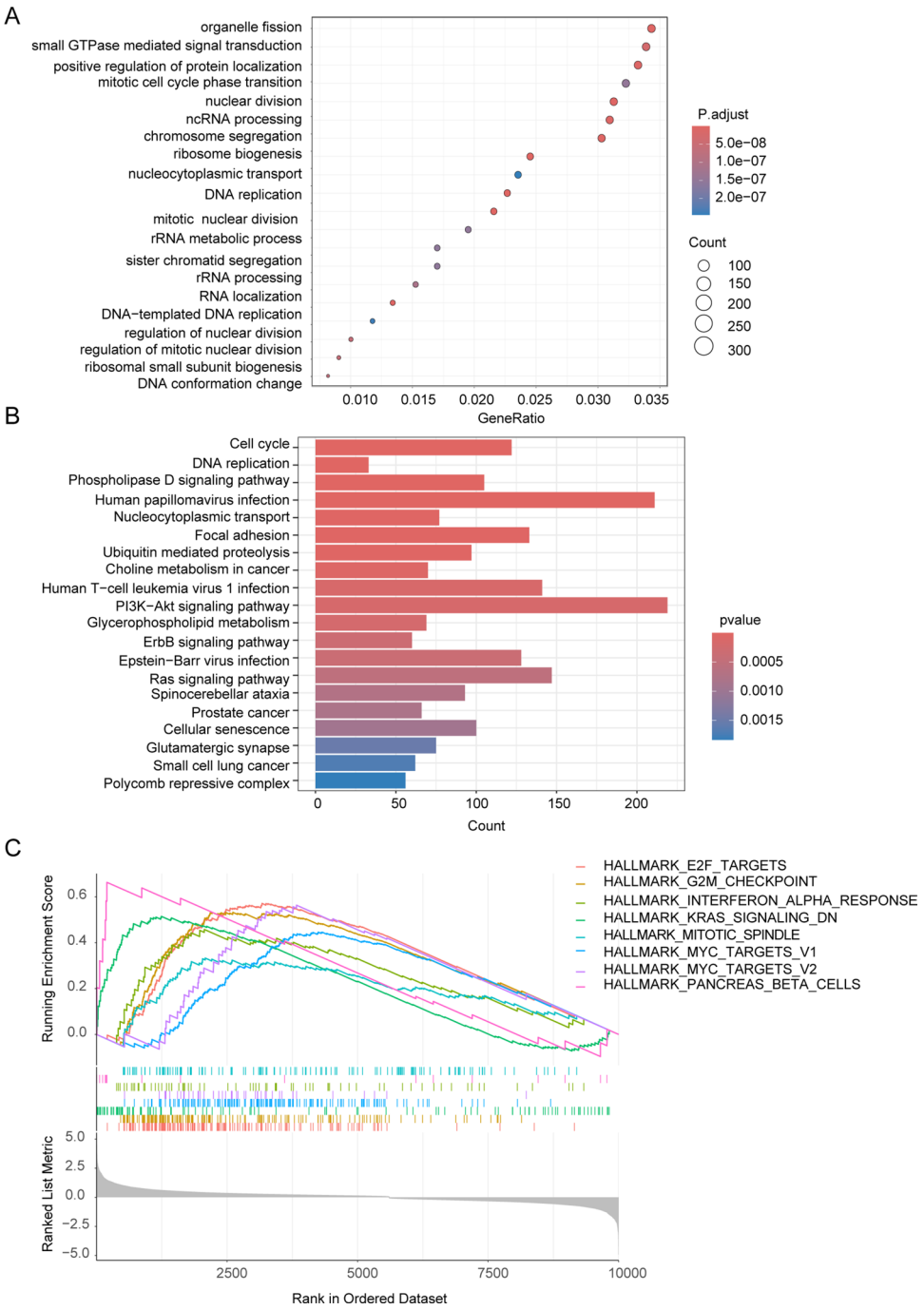

Fig. 6 The functional annotation analysis based on the signature. **A** GO functional enrichment of differentially expressed genes between two risk subgroups in the entire set. **B** KEGG pathways enrichment of differentially expressed genes between two risk subgroups in the entire set. **C** GSEA results of the high-risk group versus low-risk group in prognostic signature

prognosis in the train set through univariate Cox regression analysis. Then we constructed a 16-gene lactylation-related prognostic signature through LASSO-COX algorithm. And patients in high-risk group showed a tendency to be plagued by worse prognosis. Excellent predictive performance of the signature was illustrated by the ROC curve. We verified the performance of this signature in our validation cohorts, which both showed great robustness and reliability. Moreover, the risk score as well as stage of endometrial cancer patients was proved to perform as an independent prognostic factor. Consequently, a nomogram based on age, stage, grade, and risk score was constructed to predict 1-, 3-, and 5-year OS for endometrial cancer patients which was considered to be a splendid predictive tool in clinical since its calibration curve analysis and decision curve analysis (DCA) performed well. In conclusion, our results support that this signature could accurately predict the prognosis and help make clinical decisions.

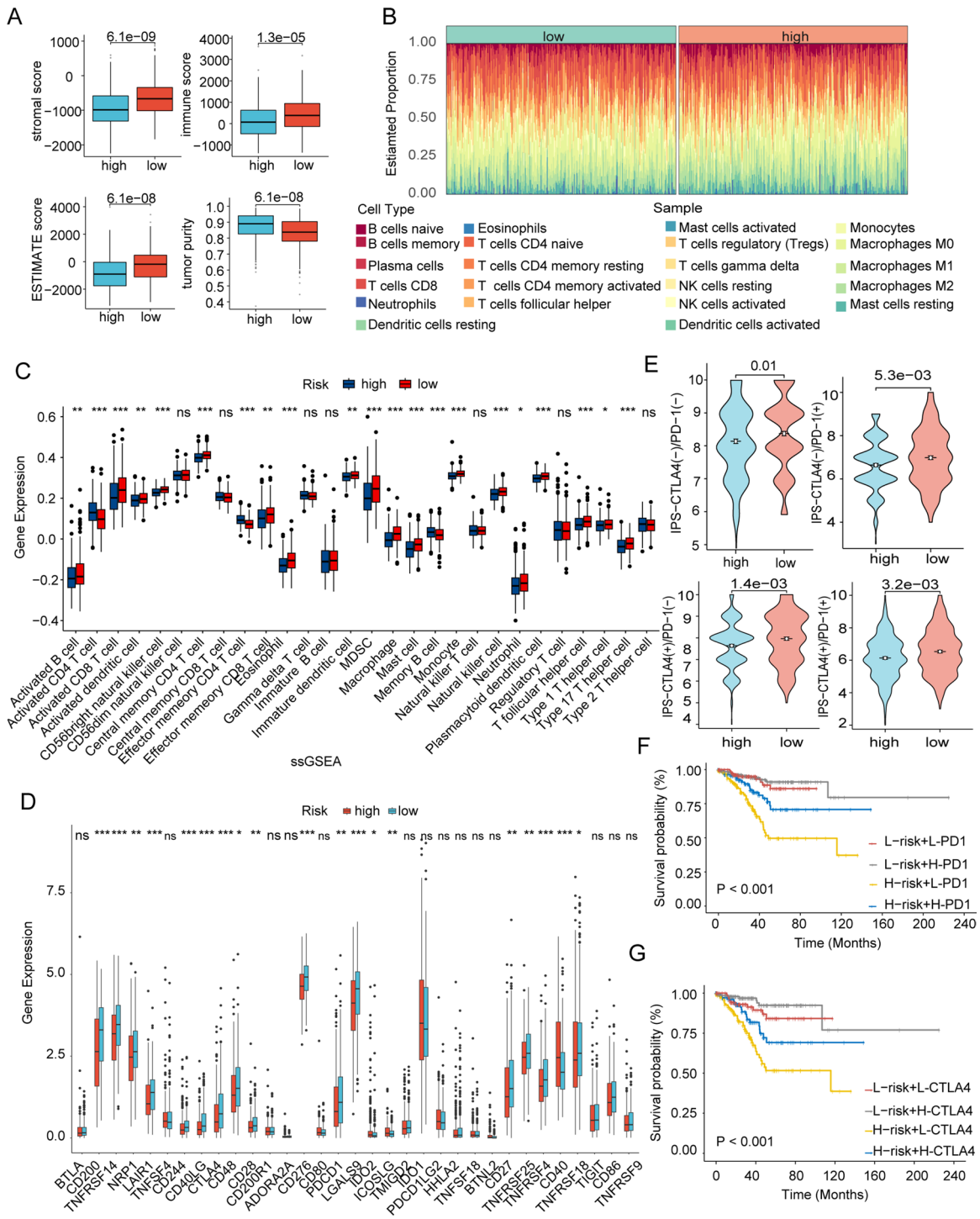

Fig. 7 The investigation of immune factors and clinical treatment in two risk groups. **A** Correlation between lactylation score and the tumor microenvironment of EC assessed using the ESTIMATE algorithm. **B** Bar chart depicting the composition of immune cells in each sample between two risk groups. **C** Violin plot illustrating the infiltration levels of different kinds of immune cells. **D** The expression of 33 immune checkpoints differs between the high-risk and low-risk groups. **E** Sensitivity analysis of the high- and low-lactylation-score groups to immunotherapy. **F** Joint survival analysis performed in the high and low-PD1 groups and the high- and low-lactylation-score groups. **G** Joint survival analysis performed in the high and low-CTLA4 groups and the high- and low-lactylation-score groups

Tumor microenvironment which encompasses infiltrating immune cells, stromal cells, and vascular cells has been

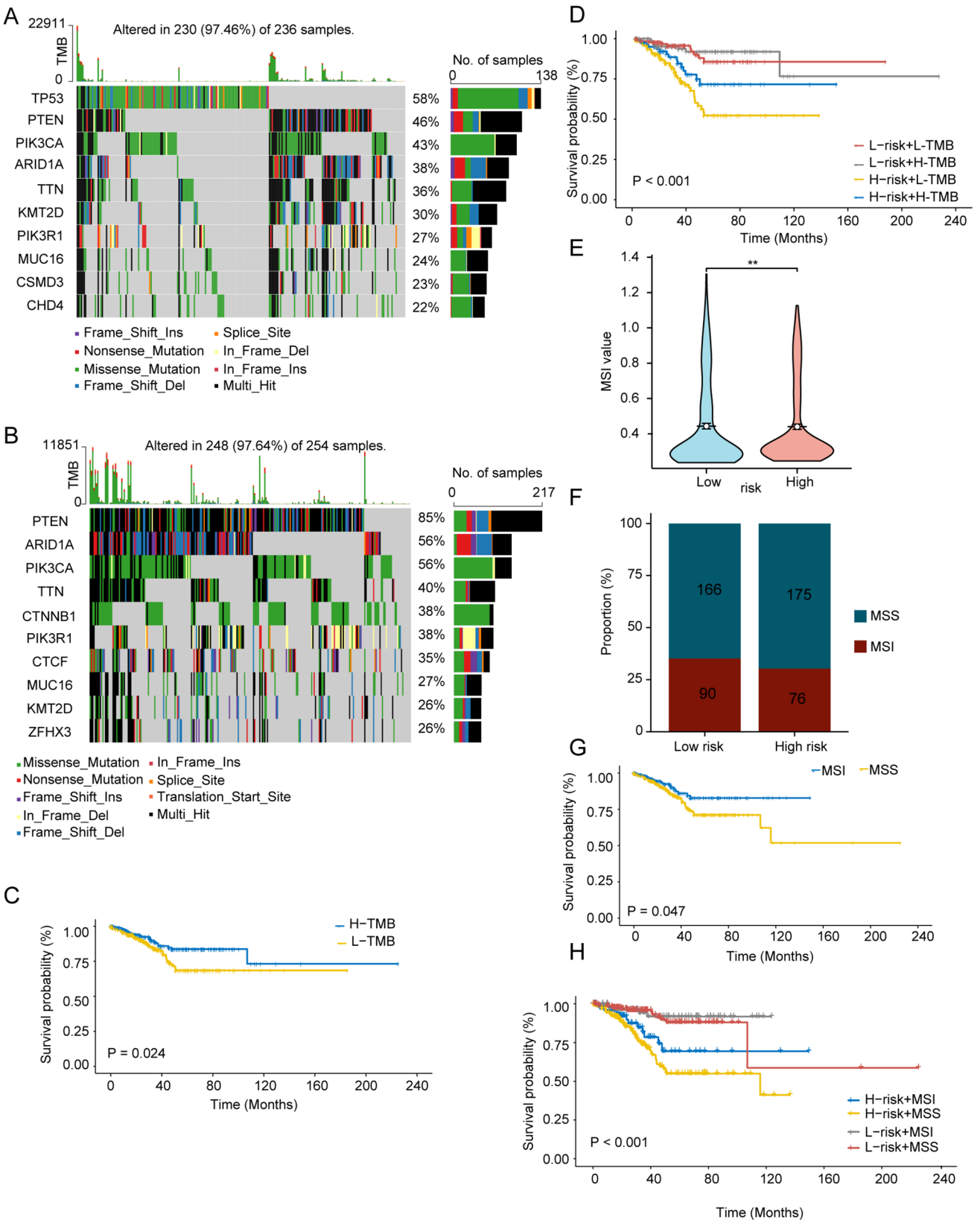

Fig. 8 Somatic mutation analysis based on the signature. **A** Waterfall plot of mutation frequencies in the high-lactylation-score group. **B** Waterfall plot of mutation frequencies in the low-lactylation-score group. **C** Kaplan–Meier survival curve of the high-tumor-mutation-burden group and the low-tumor-mutation-burden group. **D** Joint survival analysis in the high and low-tumor-mutation-burden groups and the high- and low-lactylation-score groups. **E**, **F** Differences in microsatellite instability between two risk groups. **G** Kaplan–Meier survival curve of the MSI group and the MSS group. **H** Joint survival analysis in the MSI and MSS groups and the high- and low-lactylation-score groups

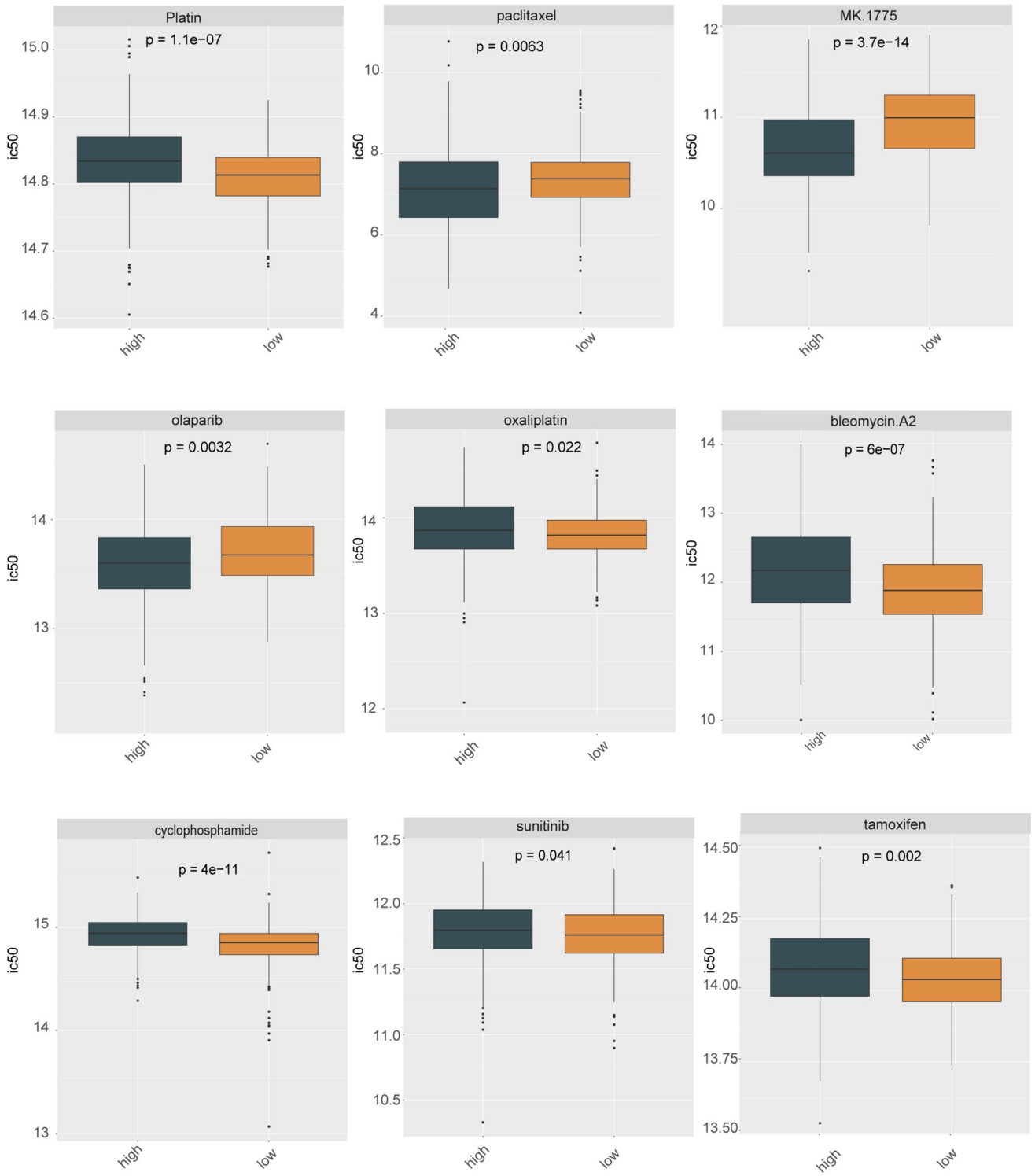

Fig. 9 Therapy sensitivity between the two risk groups

regarded as an essential mediator of tumor progression [40]. And immune and stromal cells in the TME have been proved to be associated with progression-free survival of cancer [41]. As a consequence, we explored the association between TME and the signature. Our findings indicated that a higher proportion of M1 macrophage tended to accompany with higher lactylation scores. On the contrary, low-risk group showed an quite abundance of CD8 + T cells, which might help improve survival for EC patients [42]. Immune checkpoint blockade could act as an effective therapeutic strategy

for tumors, we hence examined immune checkpoint expression in two risk groups for the purpose of predicting immunotherapy responses. The results demonstrated that several inhibitory ICIs like CTLA-4, PD-1, CD40, and CD27 were all upregulated with lower level of lactylation. And the response to ICB in both groups showed significant difference that the responders tended to belong to the low-risk group. Above results supported that the lactylation-related signature could assist to screen out a specific subset of endometrial patients with better response to immunotherapy. That is namely immunotherapy is promising for low-risk patients with higher proportion of antitumor immune-infiltrating cells.

Tumor mutational burden (TMB) has been reported to be a vital biomarker measuring the number of somatic mutations in a tumor's genome and is linked to its response to ICIs [43, 44]. To dig deeper into the molecular characteristics of lactylation in endometrial cancer, we also compared the TMB of each group. In this study, PTEN, which has been verified to be a suppressor in endometrial cancer through decreasing the activity of phosphoinositide 3-kinase (PI3K) manifested the most frequent somatic mutations in the low-risk group [45, 46]. Moreover, patients with higher TMB tended to have a better prognosis, which is concordant with other types of cancers. And the joint analysis of TMB and the lactylation score indicated that both higher level of lactylation and lower TMB were predictors of poorer prognosis in EC. Microsatellite instability has been identified in different kinds of human tumors that results from dysfunction of DNA mismatch repair-related genes [47]. We explored the relationship between MSI and lactylation-related signature. And the results revealed that the high-risk group possessed a lower MSI score. Moreover, patients with a high-risk score and MSS status had the worst prognosis compared to those in other subgroups. In addition, we compared the predicted effectiveness of other drugs between the two risk groups using GDSC dataset. We found that low-risk patients were more sensitive to platinum, tamoxifen, bleomycin, cyclophosphamide, sunitinib and oxaliplatin while high-risk patients were more sensitive to paclitaxel, olaparib and MK.1775.

In conclusion, our study indicated that patients with low lactylation risk scores possessed higher IPS, higher TMB, higher MSI score, and responded more sensitively to ICIs and other drugs, which might explain the improved prognosis of the low-risk patients.

Nevertheless, there are still some limitations in our study. For one thing, our data were mainly based on TCGA cohorts, and data from more databases are still needed for validation. For another, our results lack the evidence from experiments in vitro or in vivo and we should conduct functional and mechanistic investigations to better explore the role of lactylation-related genes in the signature.

Author contributions L.C. wrote the original draft, review and editing and conducted formal analysis. M. X. finished visualization and wrote review and editing. W. W. (Weijia Wen) completed the methodology part and analysed data with software. L. Y. and Y. J. analysed data with software. X. Z., H. F. and S. L. curated data. T. L. and P. L. provided resources for this article. H. J. provided resources for this article and funded for this study. W. W. (Wei Wang) and Y. L. provided resources and funded for this article as well as supervised this study. C. Z. finished the part of conceptualization and funded for this study. S.Y. finished the part of conceptualization, provided resources and funded for this article, All authors reviewed the manuscript.

Funding This work was supported by the National Natural Science Foundation of China (82403524 to Chunyu Zhang, 82203585 to Yuandong Liao, 82273365 to Shuzhong Yao); China Postdoctoral Science Foundation (2023M744070 and 2024T17104 to Chunyu Zhang); Postdoctoral Fellowship Program of CPSF (GZC20233282 to Chunyu Zhang); Guangdong Medical Science and Technology Research Foundation (A2024280 to Chunyu Zhang); Science and Technology Plan of Guangdong Province (2023A0505050102 to Shuzhong Yao); Guangzhou Science and Technology Program (2024B03J1336 to Shuzhong Yao); Sun Yat-sen University Clinical Research Foundation of 5010 Project (2017006 to Shuzhong Yao); Guangdong Basic and Applied Basic Research Foundation (2023A1515012214 to Wei Wang, 2023A1515110333 and 2025A1515012491 to Chunyu Zhang, 2024A1515013045 to Hongye Jiang).

Data availability Data is provided within the manuscript or supplementary information files.

Declarations

Ethics approval and consent to participate This study was approved by the Ethical Review Committee of the First Affiliated Hospital of Sun Yat-sen University, the design of this study follows the tenets of the Declaration of Helsinki.

Competing interests The authors declare no competing interests.

References

1. Siegel RL, Miller KD, Fuchs HE, Jemal A. Cancer statistics, 2022. CA Cancer J Clin. 2022;72(1):7–33. https://doi.org/10.3322/caac.21708.
2. Sheikh MA, Althouse AD, Freese KE, Soisson S, Edwards RP, Welburn S, Sukumvanich P, Comerci J, Kelley J, LaPorte RE, Linkov F. USA endometrial cancer projections to 2030: should we be concerned? Fut Oncol. 2014;10(16):2561–8. https://doi.org/10.2217/fon.14.192.
3. Sung H, Ferlay J, Siegel RL, Laversanne M, Soerjomataram I, Jemal A, Bray F. Global cancer statistics 2020: GLOBOCAN estimates of incidence and mortality worldwide for 36 cancers in 185 countries. CA Cancer J Clin. 2021;71(3):209–49. https://doi.org/10.3322/caac.21660.
4. Cancer Genome Atlas Research Network, Kandoth C, Schultz N, Cherniack AD, Akbani R, Liu Y, Shen H, Robertson AG, Pashtan I, Shen R, Benz CC, Yau C, Laird PW, Ding L, Zhang W, Mills GB, Kucherlapati R, Mardis ER, Levine DA. Integrated genomic characterization of endometrial carcinoma. Nature. 2013;497(7447):67–73. https://doi.org/10.1038/nature12113.
5. Morice P, Leary A, Creutzberg C, Abu-Rustum N, Darai E. Endometrial cancer. Lancet. 2016;387(10023):1094–108. https://doi.org/10.1016/S0140-6736(15)00130-0.
6. Lee YC, Lheureux S, Oza AM. Treatment strategies for endometrial cancer: current practice and perspective. Curr Opin Obstet Gynecol. 2017;29(1):47–58. https://doi.org/10.1097/GCO.0000000000000338.
7. van den Heerik ASVM, Horeweg N, de Boer SM, Bosse T, Creutzberg CL. Adjuvant therapy for endometrial cancer in the era of molecular classification: radiotherapy, chemoradiation and novel targets for therapy. Int J Gynecol Cancer. 2021;31(4):594–604. https://doi.org/10.1136/ijgc-2020-001822.
8. Zhang D, Tang Z, Huang H, Zhou G, Cui C, Weng Y, Liu W, Kim S, Lee S, Perez-Neut M, Ding J, Czyz D, Hu R, Ye Z, He M, Zheng YG, Shuman HA, Dai L, Ren B, Roeder RG, Becker L, Zhao Y. Metabolic regulation of gene expression by histone lactylation. Nature. 2019;574(7779):575–80. https://doi.org/10.1038/s41586-019-1678-1.
9. Moreno-Yruela C, Zhang D, Wei W, Bæk M, Liu W, Gao J, Danková D, Nielsen AL, Bolding JE, Yang L, Jameson ST, Wong J, Olsen CA, Zhao Y. Class I histone deacetylases (HDAC1–3) are histone lysine delactylases. Sci Adv. 2022;8(3):eabi6696. https://doi.org/10.1126/sciadv.abi6696.
10. Zhang X, Mao Y, Wang B, Cui Z, Zhang Z, Wang Z, Chen T. Screening, expression, purification and characterization of CoA-transferases for lactoyl-CoA generation. J Ind Microbiol Biotechnol. 2019;46(7):899–909. https://doi.org/10.1007/s10295-019-02174-6.
11. Sun Y, Chen Y, Xu Y, Zhang Y, Lu M, Li M, Zhou L, Peng T. Genetic encoding of ε-N-L-lactyllysine for detecting delactylase activity in living cells. Chem Commun (Camb). 2022;58(61):8544–7. https://doi.org/10.1039/d2cc02643k.
12. Zu H, Li C, Dai C, Pan Y, Ding C, Sun H, Zhang X, Yao X, Zang J, Mo X. SIRT2 functions as a histone delactylase and inhibits the proliferation and migration of neuroblastoma cells. Cell Discov. 2022;8(1):54. https://doi.org/10.1038/s41421-022-00398-y.
13. Hagihara H, Shoji H, Otabi H, Toyoda A, Katoh K, Namihira M, Miyakawa T. Protein lactylation induced by neural excitation. Cell Rep. 2021;37(2):109820. https://doi.org/10.1016/j.celrep.2021.109820.
14. Irizarry-Caro RA, McDaniel MM, Overcast GR, Jain VG, Troutman TD, Pasare C. TLR signaling adapter BCAP regulates inflammatory to reparatory macrophage transition by promoting histone lactylation. Proc Natl Acad Sci U S A. 2020;117(48):30628–38. https://doi.org/10.1073/pnas.2009778117.
15. Sun L, Zhang Y, Yang B, Sun S, Zhang P, Luo Z, Feng T, Cui Z, Zhu T, Li Y, Qiu Z, Fan G, Huang C. Lactylation of METTL16 promotes cuproptosis via m6A-modification on FDX1 mRNA in gastric cancer. Nat Commun. 2023;14(1):6523. https://doi.org/10.1038/s41467-023-42025-8.
16. Wang T, Ye Z, Li Z, Jing DS, Fan GX, Liu MQ, Zhuo QF, Ji SR, Yu XJ, Xu XW, Qin Y. Lactate-induced protein lactylation: a bridge between epigenetics and metabolic reprogramming in cancer. Cell Prolif. 2023;56(10):e13478. https://doi.org/10.1111/cpr.13478.
17. Chen L, Huang L, Gu Y, Cang W, Sun P, Xiang Y. Lactate-lactylation hands between metabolic reprogramming and immunosuppression. Int J Mol Sci. 2022;23(19):11943. https://doi.org/10.3390/ijms231911943.
18. Xie Y, Hu H, Liu M, Zhou T, Cheng X, Huang W, Cao L. The role and mechanism of histone lactylation in health and diseases. Front Genet. 2022;13:949252. https://doi.org/10.3389/fgene.2022.949252.
19. Wan N, Wang N, Yu S, Zhang H, Tang S, Wang D, Lu W, Li H, Delafield DG, Kong Y, Wang X, Shao C, Lv L, Wang G, Tan R, Wang N, Hao H, Ye H. Cyclic immonium ion of lactyllysine reveals widespread lactylation in the human proteome. Nat Methods. 2022;19(7):854–64. https://doi.org/10.1038/s41592-022-01523-1.
20. Yu G, Wang LG, Han Y, He QY. clusterProfiler: an R package for comparing biological themes among gene clusters. OMICS. 2012;16(5):284–7. https://doi.org/10.1089/omi.2011.0118.
21. Yoshihara K, Shahmoradgoli M, Martínez E, Vegesna R, Kim H, Torres-Garcia W, Treviño V, Shen H, Laird PW, Levine DA, Carter SL, Getz G, Stemke-Hale K, Mills GB, Verhaak RG. Inferring tumour purity and stromal and immune cell admixture from expression data. Nat Commun. 2013;4:2612. https://doi.org/10.1038/ncomms3612.
22. Aran D, Sirota M, Butte AJ. Systematic pan-cancer analysis of tumour purity. Nat Commun. 2015;6:8971. https://doi.org/10.1038/ncomms9971. (**Erratum in: Nat Commun. 2016;7:10707. doi: 10.1038/ncomms10707**).
23. Newman AM, Liu CL, Green MR, Gentles AJ, Feng W, Xu Y, Hoang CD, Diehn M, Alizadeh AA. Robust enumeration of cell subsets from tissue expression profiles. Nat Methods. 2015;12(5):453–7. https://doi.org/10.1038/nmeth.3337.
24. Crosbie EJ, Kitson SJ, McAlpine JN, Mukhopadhyay A, Powell ME, Singh N. Endometrial cancer. Lancet. 2022;399(10333):1412–28. https://doi.org/10.1016/S0140-6736(22)00323-3.
25. Arend RC, Jones BA, Martinez A, Goodfellow P. Endometrial cancer: molecular markers and management of advanced stage disease. Gynecol Oncol. 2018;150(3):569–80. https://doi.org/10.1016/j.ygyno.2018.05.015.
26. Braun MM, Overbeek-Wager EA, Grumbo RJ. Diagnosis and management of endometrial cancer. Am Fam Phys. 2016;93(6):468–74.

27. Li BL, Wan XP. Prognostic significance of immune landscape in tumour microenvironment of endometrial cancer. J Cell Mol Med. 2020;24(14):7767–77. https://doi.org/10.1111/jcmm.15408.
28. Wu YL, Li JQ, Sulaiman Z, Liu Q, Wang CY, Liu SP, Gao ZL, Cheng ZP. Optimization of endometrial cancer organoids establishment by cancer-associated fibroblasts. Neoplasma. 2022;69(4):877–85. https://doi.org/10.4149/neo_2022_211110N1597.
29. Hamilton CA, Pothuri B, Arend RC, Backes FJ, Gehrig PA, Soliman PT, Thompson JS, Urban RR, Burke WM. Endometrial cancer: a society of gynecologic oncology evidence-based review and recommendations. Gynecol Oncol. 2021;160(3):817–26. https://doi.org/10.1016/j.ygyno.2020.12.021.
30. Yi L, Zhang H, Zou J, Luo P, Zhang J. Adjuvant chemoradiotherapy versus radiotherapy alone in high-risk endometrial cancer: a systematic review and meta-analysis. Gynecol Oncol. 2018;149(3):612–9. https://doi.org/10.1016/j.ygyno.2018.03.004.
31. Brooks RA, Fleming GF, Lastra RR, Lee NK, Moroney JW, Son CH, Tatebe K, Veneris JL. Current recommendations and recent progress in endometrial cancer. CA Cancer J Clin. 2019;69(4):258–79. https://doi.org/10.3322/caac.21561.
32. de la Cruz-López KG, Castro-Muñoz LJ, Reyes-Hernández DO, García-Carrancá A, Manzo-Merino J. Lactate in the regulation of tumor microenvironment and therapeutic approaches. Front Oncol. 2019;9:1143. https://doi.org/10.3389/fonc.2019.01143.
33. Rabinowitz JD, Enerbäck S. Lactate: the ugly duckling of energy metabolism. Nat Metab. 2020;2(7):566–71. https://doi.org/10.1038/s42255-020-0243-4.
34. Zhang Y, Peng Q, Zheng J, Yang Y, Zhang X, Ma A, Qin Y, Qin Z, Zheng X. The function and mechanism of lactate and lactylation in tumor metabolism and microenvironment. Genes Dis. 2022;10(5):2029–37. https://doi.org/10.1016/j.gendis.2022.10.006.
35. Cheng Z, Huang H, Li M, Liang X, Tan Y, Chen Y. Lactylation-related gene signature effectively predicts prognosis and treatment responsiveness in hepatocellular carcinoma. Pharmaceuticals (Basel). 2023;16(5):644. https://doi.org/10.3390/ph16050644.
36. Peng T, Sun F, Yang JC, Cai MH, Huai MX, Pan JX, Zhang FY, Xu LM. Novel lactylation-related signature to predict prognosis for pancreatic adenocarcinoma. World J Gastroenterol. 2024;30(19):2575–602. https://doi.org/10.3748/wjg.v30.i19.2575.
37. Huang H, Chen K, Zhu Y, Hu Z, Wang Y, Chen J, Li Y, Li D, Wei P. A multi-dimensional approach to unravel the intricacies of lactylation related signature for prognostic and therapeutic insight in colorectal cancer. J Transl Med. 2024;22(1):211. https://doi.org/10.1186/s12967-024-04955-9.
38. Mathew M, Nguyen NT, Bhutia YD, Sivaprakasam S, Ganapathy V. Metabolic signature of Warburg effect in cancer: an effective and obligatory interplay between nutrient transporters and catabolic/anabolic pathways to promote tumor growth. Cancers (Basel). 2024;16(3):504. https://doi.org/10.3390/cancers16030504.
39. Bae T, Hallis SP, Kwak MK. Hypoxia, oxidative stress, and the interplay of HIFs and NRF2 signaling in cancer. Exp Mol Med. 2024;56(3):501–14. https://doi.org/10.1038/s12276-024-01180-8.
40. Quail DF, Joyce JA. Microenvironmental regulation of tumor progression and metastasis. Nat Med. 2013;19(11):1423–37. https://doi.org/10.1038/nm.3394.
41. Mahajan UM, Langhoff E, Goni E, Costello E, Greenhalf W, Halloran C, Ormanns S, Kruger S, Boeck S, Ribback S, Beyer G, Dombroswki F, Weiss FU, Neoptolemos JP, Werner J, D'Haese JG, Bazhin A, Peterhansl J, Pichlmeier S, Büchler MW, Kleeff J, Ganeh P, Sendler M, Palmer DH, Kohlmann T, Rad R, Regel I, Lerch MM, Mayerle J. Immune cell and stromal signature associated with progression-free survival of patients with resected pancreatic ductal adenocarcinoma. Gastroenterology. 2018;155(5):1625–39. https://doi.org/10.1053/j.gastro.2018.08.009.
42. Guo F, Dong Y, Tan Q, Kong J, Yu B. Tissue infiltrating immune cells as prognostic biomarkers in endometrial cancer: a meta-analysis. Dis Markers. 2020;2020:1805764. https://doi.org/10.1155/2020/1805764.
43. Kalbasi A, Ribas A. Tumour-intrinsic resistance to immune checkpoint blockade. Nat Rev Immunol. 2020;20(1):25–39. https://doi.org/10.1038/s41577-019-0218-4.
44. Wang X, Lamberti G, Di Federico A, Alessi J, Ferrara R, Sholl ML, Awad MM, Vokes N, Ricciuti B. Tumor mutational burden for the prediction of PD-(L)1 blockade efficacy in cancer: challenges and opportunities. Ann Oncol. 2024;35(6):508–22. https://doi.org/10.1016/j.annonc.2024.03.007.
45. Bian X, Gao J, Luo F, Rui C, Zheng T, Wang D, Wang Y, Roberts TM, Liu P, Zhao JJ, Cheng H. PTEN deficiency sensitizes endometrioid endometrial cancer to compound PARP-PI3K inhibition but not PARP inhibition as monotherapy. Oncogene. 2018;37(3):341–51. https://doi.org/10.1038/onc.2017.326.
46. Xi Z, Jing L, Le-Ni K, Zhu L, Ze-Wen D, Hui Y, Ming-Rong X, Guang-Dong L. Evaluation of PTEN and CD4+FOXP3+ T cell expressions as diagnostic and predictive factors in endometrial cancer: a case control study. Medicine (Baltimore). 2019;98(30):e16345. https://doi.org/10.1097/MD.0000000000016345.
47. Arzimanoglou II, Gilbert F, Barber HR. Microsatellite instability in human solid tumors. Cancer. 1998;82(10):1808–20. https://doi.org/10.1002/(sici)1097-0142(19980515)82:10%3c1808::aid-cncr2%3e3.0.co;2-j.